

Derivative-free global ship design optimization using global/local hybridization of the DIRECT algorithm

Emilio F. Campana¹ · Matteo Diez¹ · Umberto Iemma² ·
Giampaolo Liuzzi⁴ · Stefano Lucidi³ ·
Francesco Rinaldi⁵ · Andrea Serani^{1,2}

Received: 15 October 2014 / Revised: 15 June 2015 / Accepted: 31 October 2015 /
Published online: 28 December 2015
© Springer Science+Business Media New York 2015

Abstract The application of global/local hybrid DIRECT algorithms to the simulation-based hull form optimization of a military vessel is presented, aimed at the reduction of the resistance in calm water. The specific features of the black-box-type objective function make the problem suitable for the application of DIRECT-type algorithms. The objective function is given by numerical iterative procedures, which could lead to inaccurate derivative calculations. In addition, the presence of local minima cannot be excluded a priori. The algorithms proposed (namely DIRMIN and DIRMIN-2) are hybridizations of the classic DIRECT algorithm, with deterministic derivative-free local searches. The algorithms' performances are first assessed on a

✉ Giampaolo Liuzzi
giampaolo.liuzzi@iasi.cnr.it

Emilio F. Campana
emiliofortunato.campana@cnr.it

Matteo Diez
matteo.diez@cnr.it

Umberto Iemma
umberto.iemma@uniroma3.it

Stefano Lucidi
lucidi@dis.uniroma1.it

Francesco Rinaldi
rinaldi@math.unipd.it

Andrea Serani
andrea.serani@uniroma3.it

¹ National Research Council-Marine Technology Research Institute (CNR-INSEAN),
Via di Vallerano 139, 00128 Rome, Italy

² Department of Engineering, Roma Tre University, Via Vito Volterra 62, 00146 Rome, Italy

³ Department of Computer, Control, and Management Engineering “A. Ruberti”, Sapienza
University of Rome, Via Ariosto 25, 00185 Rome, Italy

set of test problems, and then applied to the ship optimization application. The numerical results show that the local hybridization of the DIRECT algorithm has beneficial effects on the overall computational cost and on the efficiency of the simulation-based optimization procedure.

Keywords Ship design · Simulation-based design optimization · DIRECT-type algorithm · Global optimization · Local search

Mathematics Subject Classification 90C26 · 90C56 · 90C90 · 49Q10

1 Introduction

Simulation-based design optimization (SBDO) is an essential part of the design of complex engineering systems since the conceptual and early design stages. SBDO has been widely applied to diverse engineering fields, such as aerospace (Diez and Lemma 2012; Kotinis and Kulkarni 2012; Schillings et al. 2011), automotive (Duddeck 2008; Hojjat et al. 2014; Wang et al. 2010) and naval (Diez et al. 2012; Kandasamy et al. 2013; Papanikolaou 2010) design. SBDO methodologies generally require large computational simulations to assess the performance of a design and evaluate the relative merit of design alternatives. The constant development of SBDO methods focuses on the three essential elements: (i) the simulation capabilities and the associated accuracy of the analysis, (ii) the definition and management of the design variables, with the automatic design modification during the optimization process, and (iii) the efficiency and robustness of the optimization algorithm, which is the focus of the current work.

Within SBDO, a non-convex nonlinear programming problem of the form

$$\min_{x \in \mathcal{D}} f(x) \quad (1)$$

is solved, where $\mathcal{D} = \{x \in \mathbb{R}^n : \ell_i \leq x_i \leq u_i, i = 1, \dots, n\}$, with $-\infty < \ell_i < u_i < +\infty$ for all $i = 1, \dots, n$, and $f(x)$ is the objective function representing the performance of the engineering system under analysis and is usually of the black-box type, with values provided by computationally-expensive computer simulations. Due to the black-box nature of the objective function, derivatives are not available and function evaluations are computationally expensive. Hence, the use of numerical approximations of the derivatives might be inappropriate (i.e. too many costly function evaluations, inaccuracy of the computed values). Furthermore, in order to achieve an optimal design decision, a global minimum of $f(x)$ in the feasible domain \mathcal{D} is sought, which is motivated by the following considerations:

⁴ National Research Council-Institute for Systems Analysis and Computer Science (CNR-IASI), Via dei Taurini 19, 00185 Rome, Italy

⁵ Department of Mathematics, Padova University, Via Trieste 63, 35121 Padova, Italy

- typical objective functions are very often non-convex and (possibly) multi-modal, so that local minimization packages are not applicable because they could stop at a local minimum;
- the ever advancing work of design engineers has led to the production of approximately locally optimal configurations so that the margin for improvements is rapidly narrowing, and the possibility that further improvements could come from local optimization methods with small design variations is likely getting small.

The objective of the present work is the efficient solution of problem (1) with a very limited budget of function evaluations, using two deterministic derivative-free (DF) local hybridizations of the DIRECT-type algorithms (Chiter 2006; Gablonsky and Kelley 2001; He et al. 2002, 2008, 2009a, b; Jones et al. 1993; Jones 2009; Liuzzi et al. 2010), which are well-behaved deterministic algorithms for global optimization and which have been successfully applied to solve several real-world problems (Bartholomew-Biggs et al. 2002; Di Serafino et al. 2011; Zhu and Bogy 2002).

DIRECT-type methods are not the only class of algorithms able to address computationally expensive black-box problems. Other deterministic and probabilistic methods could be used in the present context. In particular, we mention the mesh adaptive direct search (MADS) method (Audet and Dennis 2006; Audet et al. 2008), particle swarm algorithms (Chen et al. 2015; Serani et al. 2014), genetic algorithms (Deb et al. 2002), and simulated annealing (Kirkpatrick et al. 1983; Kirkpatrick 1984) codes. However, the deterministic nature of DIRECT, which does not require statistical analyses of the optimization results, along with the promising outcomes of earlier research, motivate the choice of the current investigation.

Specifically, DIRMIN (Liuzzi et al. 2010, 2015) and a modification thereof, namely DIRMIN-2, are studied in order to determine the most promising algorithm parameter settings. The performance of DIRMIN and DIRMIN-2 is influenced mainly by the choice of two parameters: (a) an activation trigger, which defines when the DF local minimization starts in terms of algorithm's iteration, and (b) a tolerance used to define the DF local searches accuracy. The sensitivity of the algorithms to the two parameters is studied by using 25 different parameter combinations and applying the algorithms to 72 analytical test functions that have a level of complexity and dimensionality similar to typical optimization problems in ship design. Data and performance profiles (Moré and Wild 2009), along with three absolute metrics (Serani et al. 2014), are assessed to identify the most significant algorithm parameters. The most promising implementations are applied to a ship SBDO problem.

The SBDO application pertains to the hull-form optimization of a USS Arleigh Burke-class destroyer, namely the DDG-51. The DTMB 5415 model, an open-to-public early concept of the DDG-51, is used in the current study. The DTMB 5415 model has been widely investigated through towing tank experiments (Irvine et al. 2008; Longo and Stern 2005; Stern et al. 2000) and hull-form SBDO (Campana et al. 2006; Kandasamy et al. 2014; Serani et al. 2015; Tahara et al. 2008). Lately,

the DTMB 5415 model has been selected as the test case for the SBDO activities within the NATO STO AVT-204 “Assess the Ability to Optimize Hull Forms of Sea Vehicles for Best Performance in a Sea Environment”, aimed at multi-objective design optimization for multi-speed reduced resistance and improved seakeeping performance (Diez et al. 2015b). Herein, a single-speed single-objective SBDO example is presented, aimed at the reduction of the total resistance in calm water at 18 kn, corresponding to a Froude number (Fr) equal to 0.25; 8 variables are used for the shape modification and the analysis tool used for the current test is a potential flow solver. Each function evaluation takes about 10 min on an 8 core workstation.

2 The DIRECT algorithm

DIRECT is a sampling deterministic global derivative-free optimization algorithm and a modification of the Lipschitzian optimization method (Jones et al. 1993). It starts the optimization by transforming the domain \mathcal{D} of the problem into the unit hyper-cube D . At the first step of DIRECT, $f(x)$ is evaluated at the center (c) of the search domain; the hyper-cube is then partitioned into a set of smaller hyper-rectangles and $f(x)$ is evaluated at their centers. Let the partition of D at iteration k be defined as

$$\mathcal{H}_k = \{D_i : i \in \mathcal{I}_k\}, \text{ with } D_i = \{x \in \mathbb{R}^n : \ell_j^{(i)} \leq x_j \leq u_j^{(i)}, j = 1, \dots, n, \forall i \in \mathcal{I}_k\} \quad (2)$$

where n is the number of design variables, $\ell_j^{(i)}$ and $u_j^{(i)} \in [0, 1]$, with $i \in \mathcal{I}_k$, are the lower and upper bounds defining the hyper-rectangle D_i , and \mathcal{I}_k is the set of indices identifying the subsets defining the current partition. At a generic k th iteration of the algorithm, starting from the current partition \mathcal{H}_k of D , a new partition, \mathcal{H}_{k+1} , is built by subdividing a set of promising hyper-rectangles of the previous one. The identification of “potentially optimal” hyper-rectangles is based on some measure of the hyper-rectangle itself and on the value of $f(x)$ at its center c^i . The refinement of the partition continues until a prescribed number of function evaluations have been performed, or another stopping criterion is satisfied. The minimum of $f(x)$ over all the centers of the final partition, and the corresponding centers, provide an approximate solution to the problem.

3 The DIRMIN algorithm

DIRMIN is a hybridization of the DIRECT algorithm with a DF local search algorithm. The DF local searches are performed starting from the centers c^i of the “potentially optimal” hyper-rectangles identified by DIRECT methods. The DIRMIN algorithm, recalled from Liuzzi et al. (2015), is reported in the following:

Algorithm DIRMIN

$\mathcal{H}_k = \{D\}$, with $k = 0$, $c = \text{center of } D$, $f_{\min} = f(c)$, $x_{\min} = \{c\}$, $\beta > 0$, $\gamma \in [0, 1]$, $N_{\max} \geq 0$

Repeat

(S.1) Set $k = k + 1$, identify the potentially optimal hyper-rectangles \mathcal{P}_k in \mathcal{H}_{k-1} and set $f_{\text{mold}} = f_{\min}$

(S.2) **If** (function evaluations $\geq \gamma \cdot N_{\max}$) **then**
 for all centroids c^i of hyper-rectangles in \mathcal{P}_k perform a local minimization until the maximum step-length becomes smaller than the tolerance β , and record the best function value f_{ml}
else set $f_{\text{ml}} = +\infty$

(S.3) subdivide the potentially optimal hyper-rectangles to build \mathcal{H}_k

(S.4) evaluate f at the centers of the new hyper-rectangles

(S.5) $f_{\min} = \min \{f_{\text{mold}}, f_{\text{ml}}, \min\{f(c) : c \in C_k\}\}$, $x_{\min} \in \{x \in D : f(x) = f_{\min}\}$
 C_k is the set of centroids c of the hyper-rectangles in \mathcal{H}_k

Until (function evaluations $> N_{\max}$)

Return f_{\min} , x_{\min}

Here, D represents the unit hyper-cube, β is the tolerance used in the stopping criterion of the DF local minimizations, γ is the activation trigger defining the starting point of the DF local searches as ratio of the maximum number of function evaluation N_{\max} , and f_{ml} is the minimum value found by the DF local searches. At each iteration k , every hyper-rectangle in \mathcal{H}_k is characterized by the length of its diagonal and the value of the objective function at its centroid. Hence, provided that the Lipschitz constant is known, for every hyper-rectangle it is possible to compute a lower bound. An hyper-rectangle is declared potentially optimal (\mathcal{P}_k) and then selected for further subdivision if an estimate $L > 0$ of the Lipschitz constant exists such that it yields the best estimated lower bound among all the hyper-rectangles. The subdivision performed in Step (S.3) is carried out by dividing the hyper-rectangles along the longest edges, thus guaranteeing that the hyper-rectangles shrink on every dimension in a sufficiently balanced way.

The local minimizations at Step (S.2) are performed by using the DF local optimization algorithm for bound constrained problems proposed by Lucidi and Sciandrone (2002). It performs derivative-free line searches along the coordinate directions. At every iteration, the maximum of the step-lengths gives a measure of stationarity of the current iterate (see e.g. Kolda et al. 2003) and motivates the stopping criterion adopted at Step (S.2) of DIRMIN. As shown by Liuzzi et al. (2015), the DIRMIN algorithm can be efficient, in terms of function evaluations, with respect to the original DIRECT algorithm. The maximum number of function evaluations is used as stopping criterion of DIRMIN. It should be noted that the DIRECT algorithm is obtained from DIRMIN by simply replacing Step (S.2) with the assignment $f_{\text{ml}} = +\infty$.

4 The DIRMIN-2 algorithm

DIRMIN-2 is a modification of DIRMIN. Rather than performing the DF local minimizations starting from the centroids of all the potentially optimal hyper-rectangles \mathcal{P}_k , a single DF local minimization is performed starting from the best point produced by dividing the potentially optimal hyper-rectangles. The DF local optimization algorithm proposed by Lucidi and Sciandrone (2002) is used. Details of DIRMIN-2 are given below.

Algorithm DIRMIN-2

$\mathcal{H}_k = \{D\}$, with $k = 0$, $c =$ center of D , $f_{\min} = f(c)$, $x_{\min} = \{c\}$, $\beta > 0$, $\gamma \in [0, 1]$, $N_{\max} \geq 0$

Repeat

- (S.1) Set $k = k + 1$, identify the potentially optimal hyper-rectangles \mathcal{P}_k in \mathcal{H}_{k-1} and set $f_{\text{mold}} = f_{\min}$
- (S.2) subdivide the potentially optimal hyper-rectangles to build \mathcal{H}_k
- (S.3) evaluate f at the centers of the new hyper-rectangles
- (S.4) let $\tilde{c} \in \arg \min\{f(c) : c \in C_k\}$, where C_k the set of the centers of the hyper-rectangles \mathcal{H}_k
- (S.5) **If** (function evaluations $\geq \gamma \cdot N_{\max}$) **then**
 perform a local minimization starting from \tilde{c}
 until the maximum step-length becomes smaller than the tolerance β ,
 and let f_{ml} be the best function value found
else set $f_{\text{ml}} = +\infty$
- (S.6) $f_{\min} = \min\{f_{\text{mold}}, f_{\text{ml}}, \min\{f(c) : c \in C_k\}\}$, $x_{\min} \in \{x \in D : f(x) = f_{\min}\}$

Until (function evaluations $> N_{\max}$)

Return f_{\min} , x_{\min}

Note that, when $\arg \min\{f(c) : c \in C_k\}$ is not a singleton, \tilde{c} is the centroid of the first hyperrectangle (among those produced at step S.2) for which $f(\tilde{c}) = \min\{f(c) : c \in C_k\}$. The rationale behind the definition of DIRMIN-2 hinges on considering the subdivision of potentially optimal hyper-rectangles as a crude kind of local search, which can be improved by the use of a more sophisticated and efficient local minimization algorithm.

Also in this case, the DIRECT algorithm is obtained from DIRMIN-2 by simply replacing Step (S.4) and (S.5) with the assignment $f_{\text{ml}} = +\infty$.

5 Evaluation metrics

The metrics used to assess the performance and identify the most promising setup of DIRMIN and DIRMIN-2 are presented in the following.

5.1 Performance and data profiles

In order to evaluate the relative performance of the proposed algorithms, the procedure proposed by Moré and Wild (2009) is used. The following convergence condition is applied:

$$f(x_0) - f(x_h) \geq (1 - \tau)(f(x_0) - f_L) \tag{3}$$

where

- $f(x_0)$ is the objective function value at the starting point, namely the function value at the center of the unit hyper-cube D ;
- $f(x_h)$ is the objective function value at the h th evaluation;
- $0 \leq \tau \leq 1$ is a suitably chosen tolerance;
- f_L is the smallest function value obtained by any solver within the same maximum computational budget.

The main concepts needed to formally define data and performance profiles are recalled in the following. Let \mathcal{A} be a set of $|\mathcal{A}|$ algorithms, and \mathcal{P} a set of $|\mathcal{P}|$ problems and a performance measure $m_{p,a}$. In this work, $m_{p,a}$ is the number of function evaluations needed for algorithm a to satisfy (3) on problem p . The performance on problem p by algorithm a is compared with the best performance by any algorithm on this problem, using the following *performance ratio*:

$$r_{p,a} = \frac{m_{p,a}}{\min\{m_{p,a} : a \in \mathcal{A}\}} \tag{4}$$

Thus, a first measure of the performance of algorithm a is defined by the *performance profile*:

$$\rho_a(\alpha) = \frac{1}{|\mathcal{P}|} \text{size } \{p \in \mathcal{P} : r_{p,a} \leq \alpha\} \tag{5}$$

which approximates the probability for algorithm $a \in \mathcal{A}$ that the performance ratio $r_{p,a}$ is within a factor $\alpha \in \mathbb{R}$ of the best possible ratio. The convention $r_{p,a} = \infty$ is used when algorithm a fails to satisfy the convergence test (3) for problem $p \in \mathcal{P}$. We remark that performance profiles are plotted for values of the performance ration α such that

$$1 \leq \alpha \leq 1.1 \max_{p \in \mathcal{P}, a \in \mathcal{A}} r_{p,a}.$$

A further measure of the algorithms' performance is given by the percentage of problems that can be solved (for a given tolerance τ) within a certain number of v simplex gradient evaluations. Namely, the so called *data profile* is defined as:

$$d_a(v) = \frac{1}{|\mathcal{P}|} \text{size } \{p \in \mathcal{P} : \frac{m_{p,a}}{n_p + 1} \leq v\} \tag{6}$$

where n_p is the number of variables in $p \in \mathcal{P}$. If the convergence test (3) cannot be satisfied within the assigned computational budget, $m_{p,a}$ is set equal to ∞ . We again remark that data profiles are plotted for values of v such that

$$0 \leq v \leq 1.1 \max_{p \in \mathcal{P}, a \in A} \frac{m_{p,a}}{n_p + 1}.$$

5.2 Absolute metrics

Three absolute performance criteria are used to further assess the algorithms and defined as follows (Serani et al. 2014):

$$\Delta_x = \sqrt{\frac{1}{n} \sum_{i=1}^n \left(\frac{x_{i,\min} - x_{i,\min}^*}{R_i} \right)^2}, \quad \Delta_f = \frac{f_{\min} - f_{\min}^*}{f_{\max}^* - f_{\min}^*}, \quad \Delta_t = \sqrt{\frac{\Delta_x^2 + \Delta_f^2}{2}} \quad (7)$$

Δ_x is a normalized Euclidean distance between the minimum position found by the algorithm (x_{\min}) and the analytical minimum position (x_{\min}^*), where $R_i = |u_i - l_i|$ is the range of the i th variable. Δ_f is the associated normalized distance in the image space, f_{\min} is the minimum found by the algorithm, f_{\min}^* is the analytical minimum, and f_{\max}^* is the analytical maximum of the function $f(x)$ in the search domain \mathcal{D} . Δ_t is a combination of Δ_x and Δ_f and used for an overall assessment.

Additionally, the relative variability $\sigma_{r,k}^2$ for each metric $\Delta_x, \Delta_f, \Delta_t$ (Eq. 7) is used to assess the impact of each tuning parameter s_k on the algorithms' performance. Defining the algorithm's tuning parameter vector as $s = [s_1, s_2, \dots, s_S]^T \in \mathbb{R}^S$, the relative performance variability associated to its k th component is

$$\sigma_{r,k}^2 = \frac{\sigma_k^2}{\sum_{k=1}^S \sigma_k^2} \quad (8)$$

where

$$\sigma_k^2 = \frac{1}{|\Omega|} \sum_{\omega \in \Omega} [\hat{\Delta}_k(\omega)]^2 - \left[\frac{1}{|\Omega|} \sum_{\omega \in \Omega} \hat{\Delta}_k(\omega) \right]^2 \quad (9)$$

with Ω containing the positions ω assumed by the parameter s_k ,

$$\hat{\Delta}_k(\omega) = \frac{1}{|\mathcal{B}|} \sum_{s \in \mathcal{B}} \bar{\Delta}(s), \quad \mathcal{B} = \{s : s_k = \omega\} \quad (10)$$

and

$$\bar{\Delta}(s) = \frac{1}{|\mathcal{P}|} \sum_{p \in \mathcal{P}} [\Delta(s)]_p. \quad (11)$$

6 Optimization problems

The analytical test problems and the ship design problem used to assess the performance of DIRMIN and DIRMIN-2 are presented in the following.

6.1 Analytical test problems

The test problems used herein have been used in earlier work (Liuzzi et al. 2015; Serani et al. 2014) and summarized in Table 1. They include unimodal functions (i.e., those denoted by a superscript “*” in Table 1), highly-complex multimodal functions and non-differentiable problems, with n ranging from 2 to 50. The analytical expressions of the test functions are reported in Appendix.

A limit on the maximum number of function evaluations N_{\max} is imposed equal to 256 n . The DF local minimizations in DIRMIN and DIRMIN-2 start when the number of function evaluations reaches the activation trigger γN_{\max} , where $\gamma \in [0, 1]$. The local minimizations proceed until either the number of function evaluations exceeds N_{\max} or the stepsize falls below the given tolerance $\beta > 0$. The values that can be assumed by the parameters γ and β are summarized in Table 2. The algorithms with the respective parameter value combinations are numbered from 1 to 25.

6.2 Ship design problem

The hull-form optimization of the DTMB 5415 model is solved for resistance reduction. Figure 1 shows the geometry of a 5.720 m length model used for towing tank experiments, as seen at CNR-INSEAN (Stern et al. 2000). The main particulars of the full scale model and the test conditions are summarized in Tables 3 and 4, respectively.

The objective function is the reduction of the total resistance (R_T) in calm water at Fr equal to 0.25. An orthogonal representation of the shape modification vector $\delta \in \mathbb{R}^3$ is used (Serani et al. 2015), since it has been shown to be more efficient in the context of shape design optimization (Diez et al. 2015a). Specifically, 8 orthogonal functions $\psi_j \in \mathbb{R}^3$ ($j = 1, \dots, 8$) are applied for the modification of the hull shape, controlled by 8 design variables $\alpha_j \in \mathbb{R}$ ($j = 1, \dots, 8$), as

$$\delta(\xi, \eta) = \sum_{j=1}^8 \alpha_j \psi_j(\xi, \eta) \quad (12)$$

with

$$\psi_j(\xi, \eta) := \sin\left(\frac{r_j \pi \xi}{M_j - L_j} + \phi_j\right) \sin\left(\frac{t_j \pi \eta}{O_j - N_j} + \chi_j\right) e_{q(j)} \quad (13)$$

where $(\xi, \eta) \in [L_j, M_j] \times [N_j, O_j]$ are curvilinear coordinates; r_j and $t_j \in \mathbb{R}$ define the order of the function in ξ and η direction respectively; ϕ_j and $\chi_j \in \mathbb{R}$ are the corresponding spatial phases; L_j, M_j, N_j , and $O_j \in \mathbb{R}$ define the patch size; $e_{q(j)}$ is a

Table 1 Analytical test problems

f_p	Name	Dimension n	Bounds $[\ell_i, u_i], i = 1, \dots, n$	Optimum f_{\min}
f_1	Sphere*	2	$[-5, 4]^n$	0.000
f_2	Freudenstein–Roth	2	$[-5, 5]^n$	0.000
$f_{3,4,5,6}$	Ackley	2, 10, 30, 50	$[-5, 4]^n$	0.000
f_7	Three-Hump Camel Back	2	$[-5, 4]^n$	0.000
f_8	Six-Hump Camel Back	2	$[-2.5, 2.5] \times [-1.5, 1.5]$	-1.032
f_9	Quartic*	2	$[-10, 10]^n$	-0.352
f_{10}	Beale	2	$[-4.5, 4.5]^n$	0.000
f_{11}	Shubert penalty 1	2	$[-10, 10]^n$	-186.731
f_{12}	Shubert penalty 2	2	$[-10, 10]^n$	-186.731
f_{13}	Booth*	2	$[-10, 10]^n$	0.000
f_{14}	Matyas*	2	$[-9, 7]^n$	0.000
f_{15}	Goldstein–Price	2	$[-2, 2]^n$	3.000
f_{16}	Bukin n.6	2	$[-15, -5] \times [-3, 3]$	0.000
f_{17}	Rosenbrock*	2	$[-100, 100]^n$	0.000
f_{18}	Schaffer n.2	2	$[-100, 90]^n$	0.000
f_{19}	Schaffer n.6	2	$[-100, 90]^n$	0.000
f_{20}	Easom	2	$[-100, 100]^n$	-1.000
f_{21}	Test Tube Holder	2	$[-10, 10]^n$	-10.872
f_{22}	Treccani*	2	$[-5, 4]^n$	0.000
f_{23}	Tripod	2	$[-100, 100]^n$	0.000
$f_{24,25}$	Exponential	2, 4	$[-9, 7]^n$	-1.000
$f_{26,27}$	Styblinski–Tang	2, 4	$[-5, 5]^n$	-36.166 n
$f_{28,29}$	Cosine Mixture	2, 4	$[-1, 0.5]^n$	-0.100 n
f_{30}	Hartman n.3	3	$[0, 1]^n$	-3.860
f_{31}	Hartman n.6	6	$[0, 1]^n$	-3.320
$f_{32,33,34,35}$	5^n loc. minima (Levy)	2, 5, 10, 20	$[-10, 10]^n$	0.000
$f_{36,37,38,39}$	10^n loc. minima (Levy)	2, 5, 10, 20	$[-10, 10]^n$	0.000
$f_{40,41,42,43}$	15^n loc. minima (Levy)	2, 5, 10, 20	$[-5, 5]^n$	0.000
$f_{44,45,46,47}$	Griewank	2, 5, 10, 20	$[-9, 7]^n$	0.000
$f_{48,49,50,51}$	Alpine	2, 5, 10, 20	$[-9, 7]^n$	0.000
$f_{52,53,54,55}$	Multi Modal	2, 5, 10, 20	$[-1, 0.5]^n$	0.000
$f_{56,57,58,59,60}$	Dixon–Price*	2, 5, 10, 25, 50	$[-1, 1]^n$	0.000
f_{61}	Colville	4	$[-10, 10]^n$	0.000
f_{62}	Shekel n.5	4	$[0, 10]^n$	-10.153
f_{63}	Shekel n.7	4	$[0, 10]^n$	-10.403
f_{64}	Shekel n.10	4	$[0, 10]^n$	-10.536
$f_{65,66,67}$	Powell*	8, 16, 24	$[-4, 5]^n$	0.000
$f_{68,69,70}$	Rastrigin	10, 30, 50	$[-5.12, 5.12]^n$	0.000
$f_{71,72}$	Schwefel	10, 20	$[-500, 500]^n$	0.000

* Denotes unimodal functions

Table 2 Algorithms' setup ID

$\beta \setminus \gamma$	0.00	0.25	0.50	0.75	1.00
1e-5	1	2	3	4	5
1e-4	6	7	8	9	10
1e-3	11	12	13	14	15
1e-2	16	17	18	19	20
1e-1	21	22	23	24	25



Fig. 1 A 5.720 m length model of the DTMB 5415 (CNR-INSEAN model 2340)

Table 3 DTMB 5415 model main particulars (full scale)

Description	Symbol	Value	Unit
Displacement	∇	8636	Tonnes
Length between perpendiculars	L_{pp}	142.0	m
Beam	B	18.90	m
Draft	T	6.160	m
Longitudinal center of gravity	LCG	71.60	m
Vertical center of gravity	VCG	1.390	m

Table 4 DTMB 5145 test conditions

Description	Symbol	Value	Unit
Advancing speed	U	18.00	kn
Water density	ρ	998.5	kg/m ³
Kinematic viscosity	ν	1.09×10^{-6}	m ² /s
Gravity acceleration	g	9.803	m/s ²

unit vector. Modifications may be applied in x , y or z direction ($q(j) = 1, 2$, or 3 , respectively). Specifically, six orthogonal functions and design variables are used for the hull, whereas two functions/variables are used for the sonar dome. The corresponding functions are shown in Fig. 2. Table 5 summarized the parameters used herein, including upper and lower bounds used for the dimensional design variables α_j . The results will be presented in the following in terms of non-dimensional design variables $x_j \in [-1, 1]$ given by:

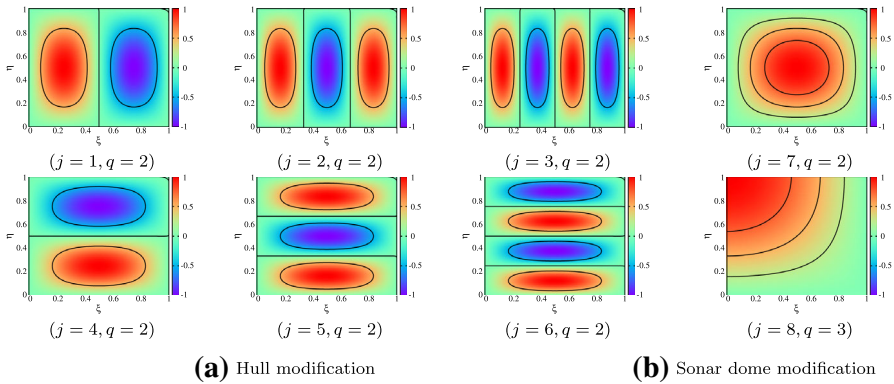


Fig. 2 Orthogonal functions $\psi_j(\xi, \eta)$ **a** Hull modification. **b** Sonar dome modification

Table 5 Orthogonal functions parameters, for shape modification

Description	j	r_j	ϕ_j	t_j	χ_j	$q(j)$	$\alpha_{j,\min}$ (m)	$\alpha_{j,\max}$ (m)
Hull Modification	1	2.0	0	1.0	0	2	-1.0	1.0
	2	3.0	0	1.0	0	2	-1.0	1.0
	3	4.0	0	1.0	0	2	-1.0	1.0
	4	1.0	0	2.0	0	2	-0.5	0.5
	5	1.0	0	3.0	0	2	-0.5	0.5
	6	1.0	0	4.0	0	2	-0.5	0.5
Sonar dome Modification	7	1.0	0	1.0	0	2	-0.3	0.3
	8	0.5	$\pi/2$	0.5	0	3	-0.5	0.5

$$x_j = 2(\alpha_j - \alpha_{j,\min}) / (\alpha_{j,\max} - \alpha_{j,\min}) - 1. \tag{14}$$

Geometrical constraints include fixed length between perpendiculars (L_{pp}) and fixed displacement (∇), with beam (B) and draft (T) varying between $\pm 5\%$ of the original value.

The solver used is the potential flow code WARP, based on the Neumann–Kelvin linearization (Bassanini et al. 1994). The wave resistance is evaluated with the transverse wave cut method (Telste and Reed 1994), whereas the friction resistance is estimated by a local approximation based on flat-plate theory (Schlichting and Gersten 2000). The steady two degrees of freedom (sinkage and trim) equilibrium is achieved by iteration of the flow solver and the body equation of motion. Simulations are performed for the right demi-hull, taking advantage of symmetry about the xz -plane. The computational domain for the free surface is defined within $1 L_{pp}$ upstream, $3 L_{pp}$ downstream and $1.5 L_{pp}$ sideways, as shown in Fig. 3a. The

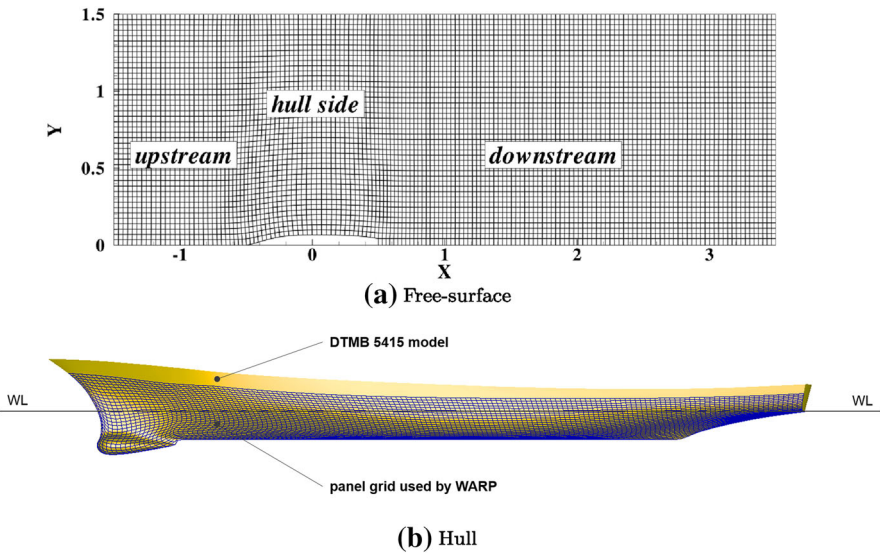


Fig. 3 Computational panel-grid. **a** Free-surface. **b** Hull

Table 6 Panel grid used for WARP

Hull	Free surface			Total
	Upstream	Hull side	Downstream	
150 × 30	30 × 44	30 × 44	90 × 44	11 k

associated panel grid used (Fig. 3b) is summarized in Table 6 and guarantee solution convergence. The validation of the potential flow analyses performed by WARP for the original hull is shown in Fig. 4 versus experimental data collected at CNR-INSEAN (Olivieri et al. 2001), showing a reasonable agreement especially for low speeds; $C_T = R_T/0.5\rho U^2 S_{w,stat}$, ζ , and τ are shown, where U is the undisturbed flow

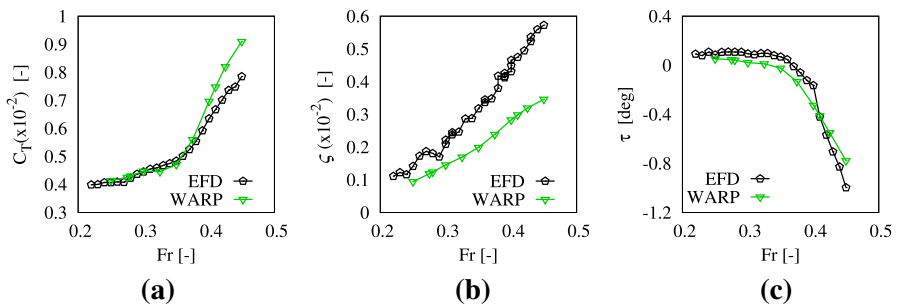


Fig. 4 Total resistance coefficient $C_T = R_T/0.5\rho U^2 S_{w,static}$ (a), non-dimensional sinkage (b), and trim (c) in calm water versus Fr, for the model scale DTMB 5415 ($L_{pp} = 5.72$ m)

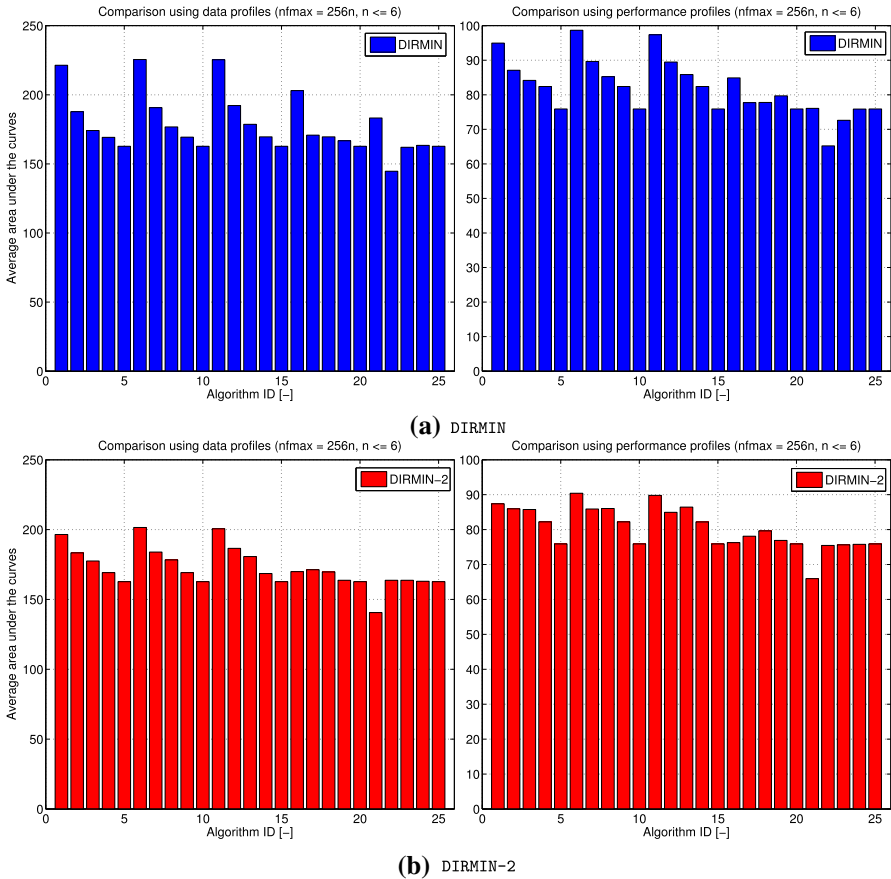


Fig. 5 Areas under the data and performance profiles for $n \leq 6$ (note that the higher the bar is, the better the algorithm)

speed, $S_{w,stat}$ is the static wetted surface area, ζ is the sinkage (positive if the center of gravity sinks), and τ is the trim angle (positive if the bow sinks).

The SBDO problem is solved by DIRECT, and the two local hybridizations DIRMIN and DIRMIN-2, setting a maximum number of function evaluations equal to 300.

7 Numerical results

The introductory study on the analytical test problems is used to identify the most promising setup for DIRMIN and DIRMIN-2. The analyses are conducted setting apart problems with less and more than six variables. The simulation-

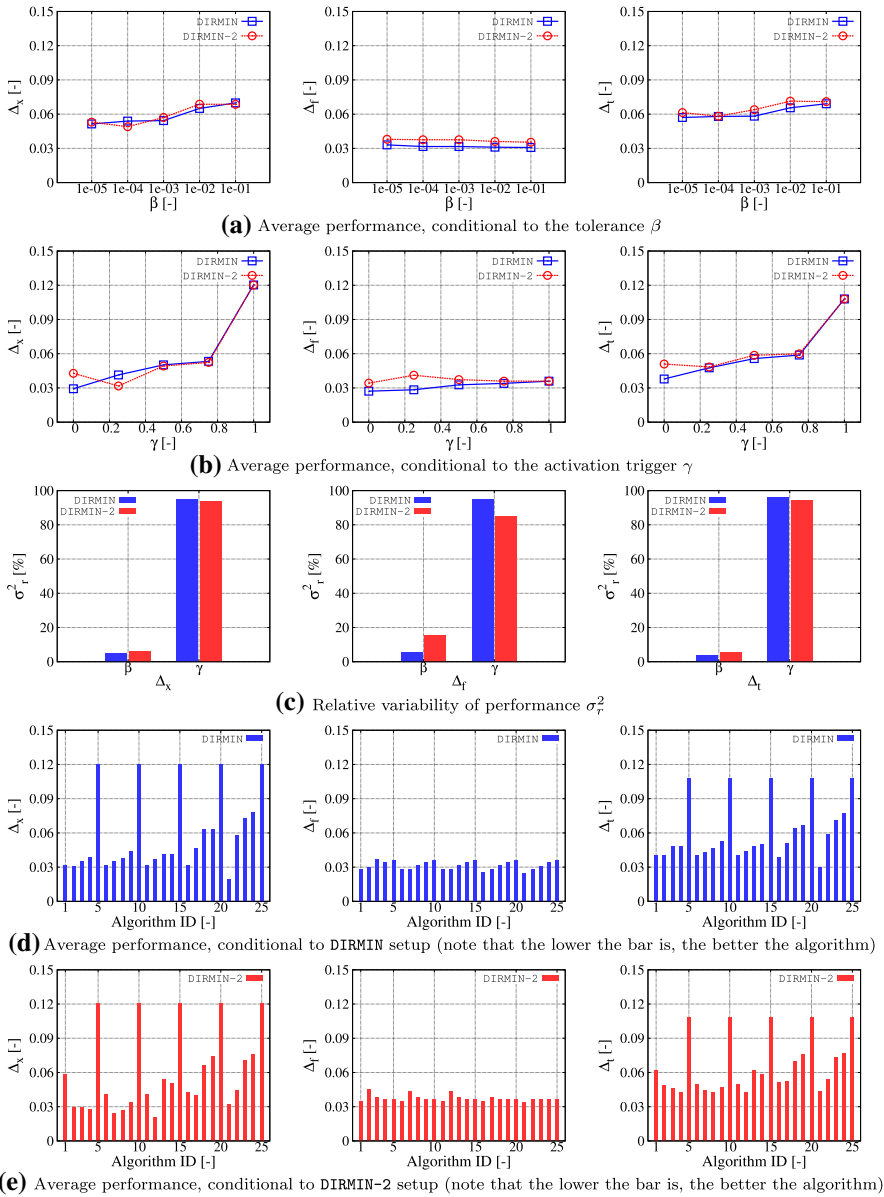


Fig. 6 Algorithms' performance for the test problems with $n \leq 6$

based design optimization of the DTMB 5415 is performed with the most promising setup of DIRMIN and DIRMIN-2 respectively, and compared with DIRECT.

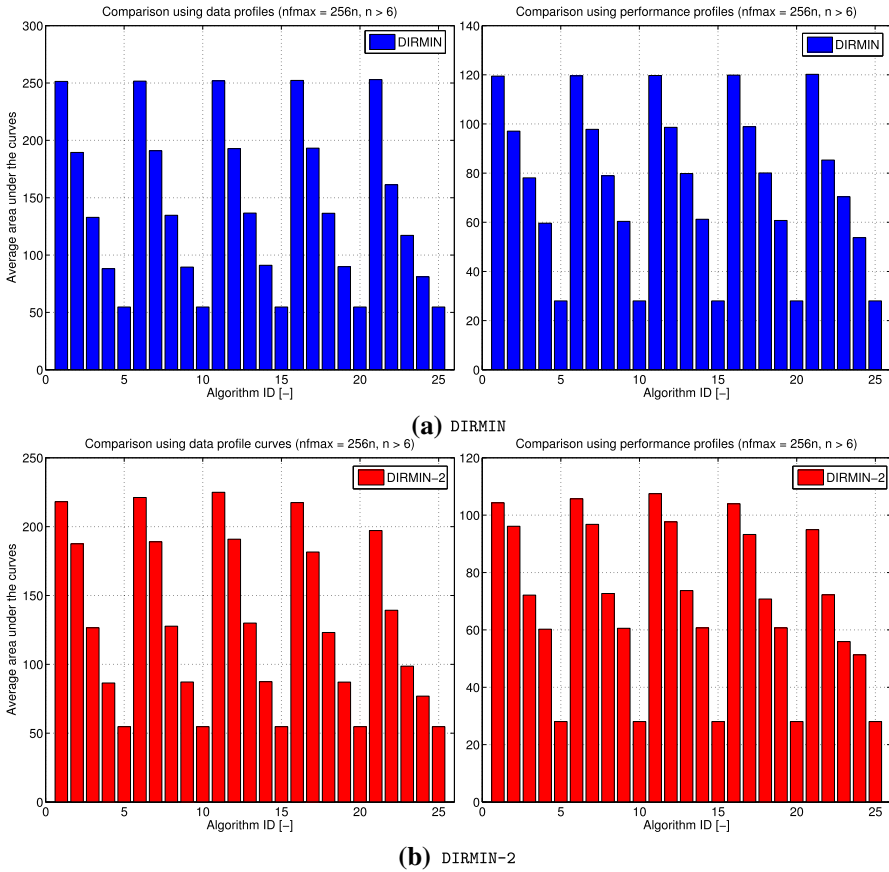


Fig. 7 Areas under the data and performance profiles for $n > 6$ (note that the higher the bar is, the better the algorithm)

7.1 Analytical test problems

Figure 5 shows the areas under data and performance profile curves of (a) DIRMIN and (b) DIRMIN-2, for the test problem with $n \leq 6$. We remark that the higher the bar is, the better the algorithm. The most promising algorithms' setup, for both DIRMIN and DIRMIN-2, appears to be setup 6, corresponding to $\gamma = 0$ and $\beta = 10^{-4}$. Figure 6a, b, show the performances of DIRMIN and DIRMIN-2 in terms of the absolute metrics Δ_x , Δ_f and Δ_t , conditional to β and γ , respectively. These results suggest starting the DF local minimizations from the very beginning ($\gamma = 0$) of the optimization procedure. Furthermore, for small problems ($n \leq 6$) a quite strict tolerance ($\beta = 10^{-4}$) for each DF local minimization is advisable. Figure 6c shows the relative variability $\sigma_{r,k}^2$ for Δ_x , Δ_f and Δ_t respectively, associated to γ and β ; γ is found the most significant parameter for both DIRMIN and DIRMIN-2. The performances of the whole set of DIRMIN and DIRMIN-2's

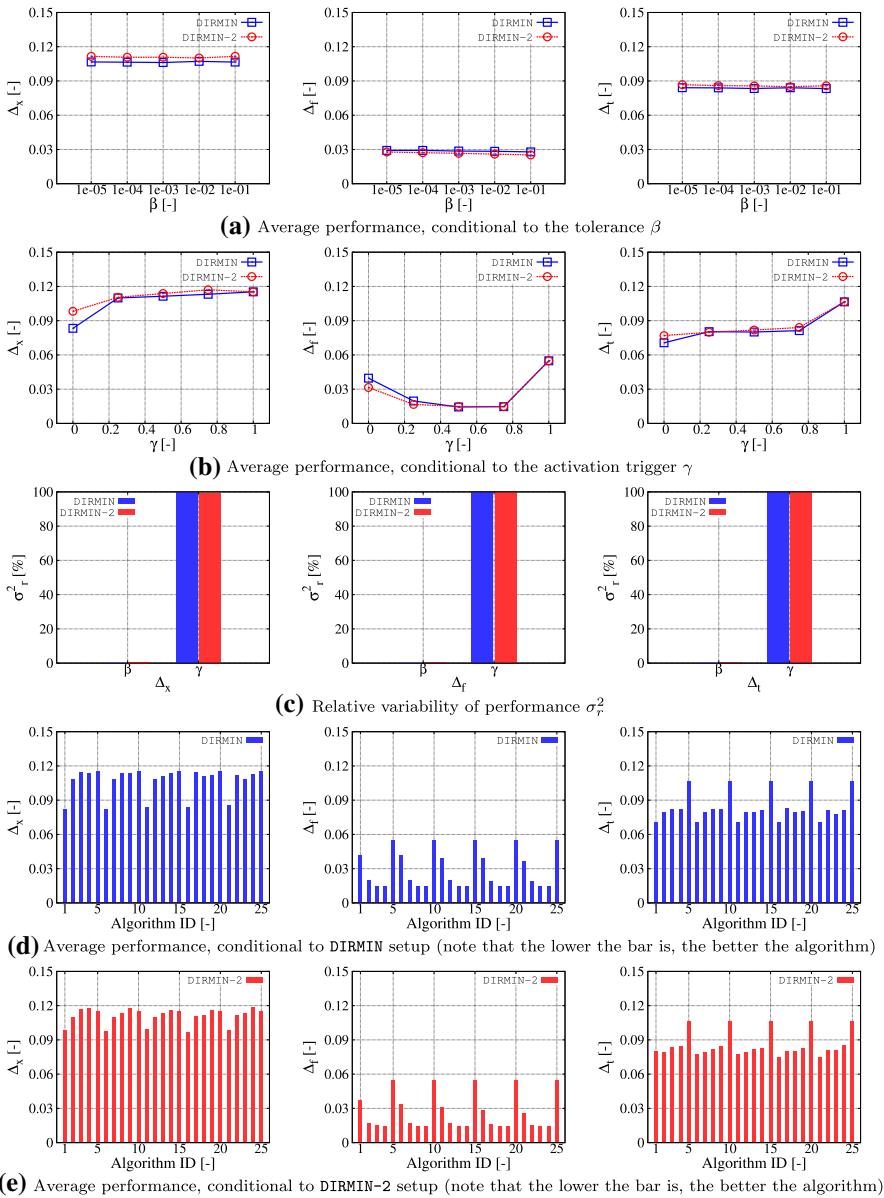


Fig. 8 Algorithms' performance for the test problems with $n > 6$

setups, in terms of Δ_x , Δ_f and Δ_t are shown in Fig. 6d, e (note that the lower the bar is, the better the algorithm), respectively. For current cases, the most promising setups based on the absolute metrics are DIRMIN(21) (i.e., $\gamma = 0$ and $\beta = 10^{-1}$) and DIRMIN-2(12) (i.e., $\gamma = 0.25$ and $\beta = 10^{-3}$).

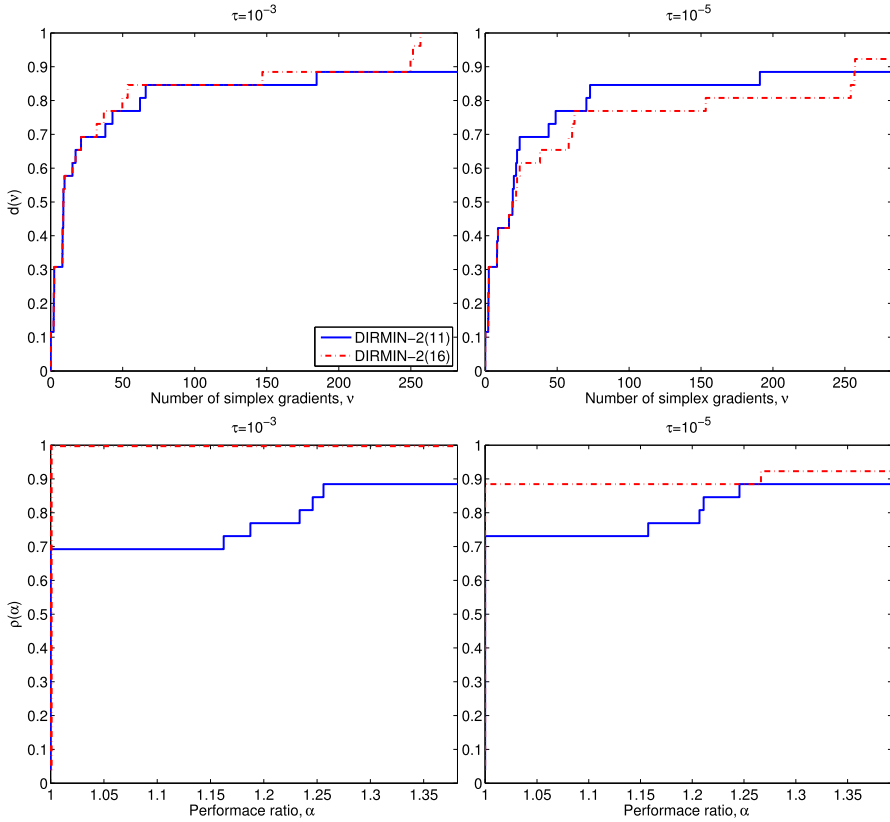


Fig. 9 Data and performance profiles for the comparison of algorithms DIRMIN-2(11) and DIRMIN-2(16)

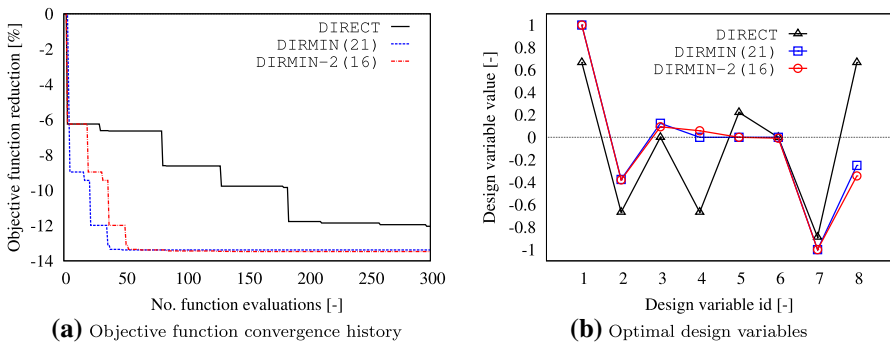


Fig. 10 Optimization results

Figure 7 shows the areas under data and performance profile curves of (a) DIRMIN and (b) DIRMIN-2, for the test problem with $n > 6$. The most promising algorithms' setups appear to be number 21 (i.e., $\gamma = 0$ and $\beta = 10^{-1}$) and 11 (i.e.,

Table 7 Summary of optimization results for DTMB 5415 model

N_{\max}	Algorithm	x_1	x_2	x_3	x_4	x_5	x_6	x_7	x_8	$R_T \times 10^5 [N]$	
										Value	$\Delta_{obj}(\%)$
300	DIRECT	0.667	-0.667	0.000	-0.667	0.222	0.000	-0.889	0.667	3.021	-12.04
	DIRECTMIN(21)	1.000	-0.375	0.125	0.000	0.000	0.000	-1.000	-0.250	2.974	-13.38
	DIRECTMIN-2(16)	1.000	-0.379	0.094	0.059	0.000	-0.008	-1.000	-0.344	2.972	-13.47

Non-dimensional design variables $x_j \in [-1, 1]$ as per Eq. 14

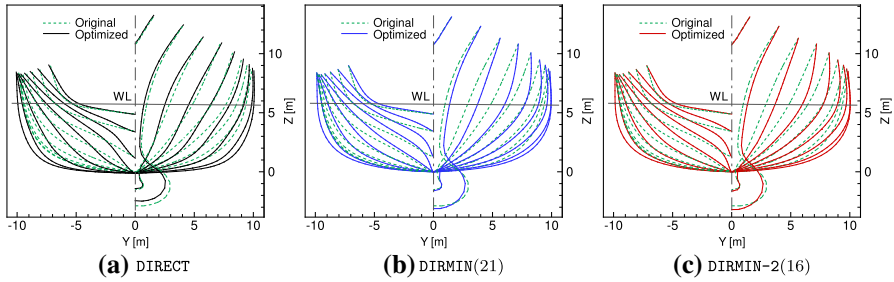


Fig. 11 Optimal hull-form shapes compared with the original for $Fr = 0.25$

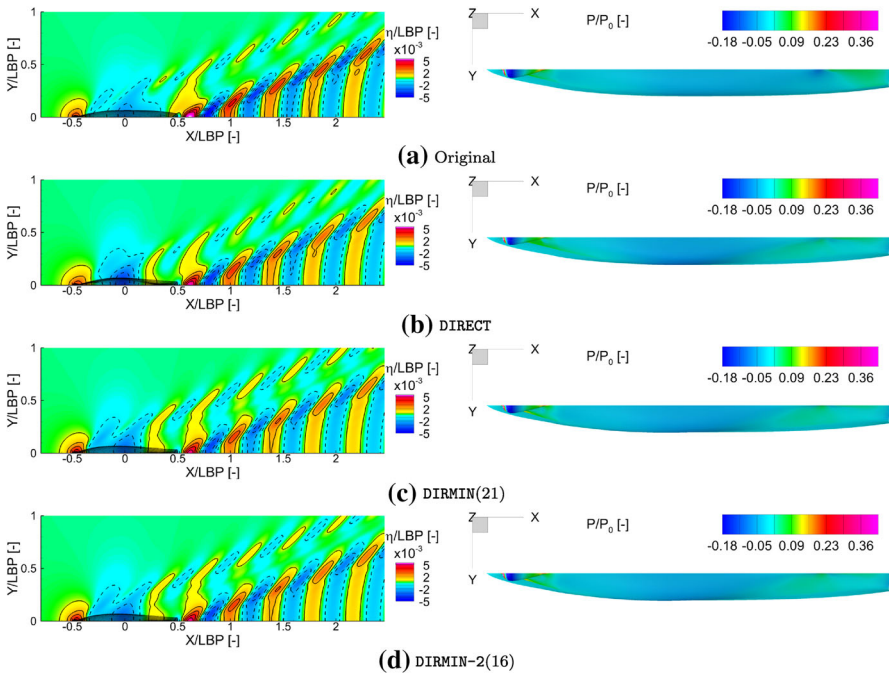


Fig. 12 Wave elevation pattern (*left*) and pressure field distribution (*right*) of the optimized hulls, compared to the original (a) for $Fr = 0.25$

$\gamma = 0$ and $\beta = 10^{-3}$) for DIRMIN and DIRMIN-2, respectively. Figure 8a, b, show the performance of DIRMIN and DIRMIN-2 in terms of the absolute metrics Δ_x , Δ_f and Δ_r , conditional to β and γ , respectively. In this case, similarly to the small problems, it is beneficial to start the local minimizations at the very beginning of the optimization procedure, whereas higher β values are more advisable, even if the relative variability (see Fig. 8c) associated with β is almost equal to zero. Also for large problems ($n > 6$), γ is found the most significant parameter. Finally, the performances of the whole set of DIRMIN and DIRMIN-2's setups, in terms of Δ_x ,

Table 8 Summary of optimization results for DTMB 5415 hull form

Parameter	Original		Optimized $\Delta\%_{orig}$		
	Value	Unit	DIRECT	DIRMIN	DIRMIN-2
C_w	1.04E-03	-	-28.3	-33.2	-33.9
C_f	1.60E-03	-	0.05	-0.06	-0.13
C_T	2.64E-03	-	-11.3	-13.2	-13.5
ζ/L_{pp}	9.42E-04	-	6.82	10.1	9.73
τ	8.99E-04	rad	105.4	150.2	144.7
$S_{w,stat}/L_{pp}^2$	1.48E-01	-	-0.85	-0.19	0.03
$S_{w,dyn}/L_{pp}^2$	1.50E-01	-	-0.80	-0.25	-0.02

Δ_f and Δ_t are shown in Fig. 8d, e (note that the lower the bar is, the better the algorithm), respectively.

The rationale behind the difference between the β s' results could be that when $n \leq 6$ some function evaluations can be devoted to achieving high precisions. This is not the case for large problems especially when considering that the adopted DF local minimizations perform a sampling along the coordinate directions thus being potentially very costly when the number of variables is large.

Finally, since the engineering application we are interested in is a problem with more than six variables, and the relative and absolute outcomes on large test problems are very similar for settings 11 and 16 of DIRMIN-2 (which are the best settings among the considered ones), we decided to further investigate the performance of DIRMIN-2(11) and DIRMIN-2(16). Performance and data profiles relative to these two versions of DIRMIN-2 are compared in Fig. 9. It can be seen that DIRMIN-2(16) is better than DIRMIN-2(11) both in terms of efficiency and robustness.

7.2 Hull-form optimization of the DTMB 5415

The SBDO procedure achieves a reduction of the objective function value by 12.04, 13.38, and 13.47 % using DIRECT, DIRMIN(21), and DIRMIN-2(16), respectively. The convergence history of the objective function is shown in Fig. 10a, confirming the efficiency of the two global/local hybrid methods, for a very limited budget of function evaluations ($N_{max} = 300$). DIRMIN and DIRMIN-2 achieve almost the final objective function reduction in the first 50 evaluations, whereas DIRECT is not able to reach the same value within the imposed limit of 300 function evaluations.

Figure 10b presents the values of the corresponding optimal design variables, showing appreciable differences for DIRECT, DIRMIN(21), and DIRMIN-2(16). Optimal design variable value and objective function reductions are summarized in Table 7. Figure 11 shows the sections of the optimized hull compared to the original. The reduction of the total resistance is consistent with the reduction of the wave elevation patterns, both in terms of transverse and diverging Kelvin waves, as shown in Fig. 12a. Figure 12b shows the pressure field on the optimized hulls

compared to the original, showing a slightly better pressure recovery towards the stern.

Finally, Table 8 summarizes the main parameters associated with the optimal DIRECT, DIRMIN(21), and DIRMIN-2(16) designs. The resistance coefficients are defined as $C_x = R_x / 0.5\rho U^2 S_{w,stat}$, with R_w , R_f , R_T being the wave, frictional and total resistance, respectively; $S_{w,stat}$ and $S_{w,dyn}$ are the static and dynamic wetted surface areas.

8 Conclusions

A simulation-based derivative-free global optimization of the hull-form design of a military vessel (namely the DTMB 5415 model) has been shown, based on global/local hybridizations of the DIRECT algorithm by deterministic DF local minimization. Two global/local hybrid algorithms (namely DIRMIN and DIRMIN-2) have been presented and tested on a set of 72 well-known analytical test functions, separately considering problems with $n \leq 6$ and $n > 6$ variables. The two algorithms differ in the DF local search management. In particular, while DIRMIN executes the DF local search starting from the centers of all the potentially optimal hyper-rectangles, DIRMIN-2 performs a single DF local minimization starting from the best point produced by dividing the potentially optimal hyper-rectangles.

25 different setups of the algorithms have been investigated, varying the DF local search activation trigger γ and the DF local search tolerance β . Data and performance profiles, along with absolute evaluation metrics, have been used to identify the most promising setup for both DIRMIN and DIRMIN-2. The analytical test problem results have revealed that, for both low and high dimensional problems, DIRMIN and DIRMIN-2 are mainly affected by the local search activation trigger. Specifically, the numerical experiments suggest starting the DF local searches at the beginning of the optimization procedures. Furthermore, the two hybrid algorithms are found more effective and efficient than the original DIRECT algorithm, with beneficial effects on the overall computational cost, in view of SBDO. Our study shows similar performance of DIRMIN and DIRMIN-2.

Regarding the DTMB 5415 hull-form optimization problem, DIRMIN and DIRMIN-2 have similar performances and show a significantly faster convergence than the original DIRECT algorithm. The effects of the optimization are visible in the wave elevation pattern produced by the optimized designs, consisting in a reduction of both the transverse and the diverging Kelvin waves. The optimized hull also shows a better pressure recovery towards the stern.

Future work includes the extension of global/local hybridization of the DIRECT algorithm to multi-objective problems, along with the application of higher fidelity solvers (such as Reynolds-averaged Navier–Stokes equation solvers), and design optimization based on static/dynamic metamodels (Volpi et al. 2015).

Acknowledgments The present research is supported by the US Navy Office of Naval Research Global, NICOP Grant N62909-15-1-2016, under the administration of Dr. Woei-Min Lin and Dr. Ki-Han Kim, and by the Italian Flagship Project RITMARE, coordinated by the Italian National Research Council and

funded by the Italian Ministry of Education, Research Program 2011–2013. The Authors are also indebted with three anonymous Reviewers and two Associated Editors whose comments and suggestions greatly helped to improve the paper.

Appendix: Analytical formulation of test functions

This appendix provides the analytical formulation used for the test functions of Table 1.

5^n loc. minima (Levy) function

$$f(x) = \frac{\pi}{n} \left\{ 10 \sin^2(\pi y_1) + \sum_{i=1}^{n-1} \left[(y_i - 1)^2 (1 + 10 \sin^2(\pi y_{i+1})) \right] + (y_n - 1)^2 \right\} \quad (15)$$

with $y_i = 1 + \frac{1}{4}(x_i - 1)$

10^n loc. minima (Levy) function

$$f(x) = \frac{\pi}{n} \left\{ 10 \sin^2(\pi x_1) + \sum_{i=1}^{n-1} \left[(x_i - 1)^2 (1 + 10 \sin^2(\pi x_{i+1})) \right] + (x_n - 1)^2 \right\} \quad (16)$$

15^n loc. minima (Levy) function

$$f(x) = \frac{1}{10} \left\{ \sin^2(3\pi x_1) + \sum_{i=1}^{n-1} \left[(x_i - 1)^2 (1 + \sin^2(3\pi x_{i+1})) \right] \right\} + \frac{1}{10} (x_n - 1)^2 [1 + \sin^2(2\pi x_n)] \quad (17)$$

Ackley function

$$f(x) = -20e^{-0.2\sqrt{\frac{1}{n}\sum_{i=1}^n x_i^2}} - e^{\frac{1}{n}\sum_{i=1}^n \cos(2\pi x_i)} + 20 + e \quad (18)$$

Alpine function

$$f(x) = \sum_{i=1}^n |x_i \sin(x_i) + 0.1x_i| \quad (19)$$

Beale function

$$f(x) = (1.5 + x_1 + x_1x_2)^2 + (2.25 - x_1 + x_1x_2^2)^2 + (2.625 - x_1 + x_1x_2^3)^2 \quad (20)$$

Booth function

$$f(x) = (x_1 + 2x_2 - 7)^2 + (2x_1 + x_2 - 5)^2 \quad (21)$$

Bukin No.6 function

$$f(x) = 100\sqrt{|x_2 - 0.01x_1^2|} + 0.01|x_1 + 10| \quad (22)$$

Colville function

$$f(x) = 100(x_1^2 - x_2)^2 + (x_1 - 1)^2 + (x_3 - 1)^2 + 90(x_3^2 - x_4)^2 \\ + 10.1((x_3 - 1)^2 + (x_4 - 1)^2) + 19.8(x_2 - 1)(x_4 - 1) \quad (23)$$

Cosine Mixture function

$$f(x) = -\sum_{i=1}^n \left[\frac{1}{10} \cos(5\pi x_i) - x_i^2 \right] \quad (24)$$

Dixon-Price function

$$f(x) = (x_1 - 1)^2 + \sum_{i=2}^n \left[i(2x_i^2 - x_{i-1})^2 \right] \quad (25)$$

Easom function

$$f(x) = -\cos(x_1) \cos(x_2) e^{-(x_1 - \pi)^2 - (x_2 - \pi)^2} \quad (26)$$

Exponential function

$$f(x) = -\exp\left(-\frac{1}{2} \sum_{i=1}^n x_i^2\right) \quad (27)$$

Freudenstein-Roth function

$$f(x) = (-13 + x_1 + ((5 - x_2)x_2 - 2)x_2)^2 + (-29 + x_1 + ((x_2 + 1)x_2 - 14)x_2)^2 \quad (28)$$

Goldstein-Price function

$$f(x) = \left[1 + (x_1 + x_2 + 1)^2(19 - 14x_1 + 3x_1^2 - 14x_2 + 6x_1x_2 + 3x_2^2) \right] \\ \times \left[30 + (2x_1 - 3x_2)^2(18 - 32x_1 + 12x_1^2 + 48x_2 - 36x_1x_2 + 27x_2^2) \right] \quad (29)$$

Griewank function

$$f(x) = 1 + \sum_{i=1}^n \frac{x_i}{4000} - \prod_{i=1}^n \cos(x_i/\sqrt{i}) \quad (30)$$

Hartman No.3 function

$$f(x) = - \sum_{i=1}^4 a_i \exp \left[- \sum_{j=1}^3 b_{ij} (x_j - d_{ij})^2 \right] \tag{31}$$

with

$$a = \begin{Bmatrix} 1.0 \\ 1.2 \\ 3.0 \\ 3.2 \end{Bmatrix} \quad b = \begin{Bmatrix} 3.0 & 10.0 & 30.0 \\ 0.1 & 10.0 & 35.0 \\ 3.0 & 10.0 & 30.0 \\ 0.1 & 10.0 & 35.0 \end{Bmatrix}$$

$$d = \begin{Bmatrix} 0.3689 & 0.1170 & 0.2673 \\ 0.4699 & 0.4387 & 0.7470 \\ 0.1091 & 0.8732 & 0.5547 \\ 0.03815 & 0.5743 & 0.8828 \end{Bmatrix}$$

Hartman No.6 function

$$f(x) = - \sum_{i=1}^4 a_i \exp \left[- \sum_{j=1}^6 b_{ij} (x_j - d_{ij})^2 \right] \tag{32}$$

with

$$a = \begin{Bmatrix} 1.0 \\ 1.2 \\ 3.0 \\ 3.2 \end{Bmatrix} \quad b = \begin{Bmatrix} 10.0 & 3.0 & 17.0 & 3.5 & 1.7 & 8.0 \\ 0.05 & 10.0 & 17.0 & 0.1 & 8.0 & 14.0 \\ 3.0 & 3.5 & 1.7 & 10.0 & 17.0 & 8.0 \\ 17.0 & 8.0 & 0.05 & 10.0 & 0.1 & 14.0 \end{Bmatrix}$$

$$d = \begin{Bmatrix} 0.1312 & 0.1696 & 0.5569 & 0.0124 & 0.8283 & 0.5886 \\ 0.2329 & 0.4135 & 0.8307 & 0.3736 & 0.1004 & 0.9991 \\ 0.2348 & 0.1451 & 0.3522 & 0.2883 & 0.3047 & 0.6650 \\ 0.4047 & 0.8828 & 0.8732 & 0.5743 & 0.1091 & 0.0381 \end{Bmatrix}$$

Matyas function

$$f(x) = 0.26(x_1^2 + x_2^2) - 0.48x_1x_2 \tag{33}$$

Multi Modal function

$$f(x) = \sum_{i=1}^n |x_i| \prod_{i=1}^n |x_i| \tag{34}$$

Powell function

$$f(x) = \sum_{i=2}^{n/4} \left[(x_{4i-3} + 10x_{4i-2})^2 + 5(x_{4i-1} + x_{4i})^2 + (x_{4i-2} - 2x_{4i-1})^4 + 10(x_{4i-3} - x_{4i})^4 \right] \quad (35)$$

Quartic function

$$f(x) = \frac{x_1^4}{4} - \frac{x_1^2}{2} + \frac{x_1}{10} + \frac{x_2^2}{2} \quad (36)$$

Rastrigin function

$$f(x) = 10n + \sum_{i=1}^n [x_i^2 - 10 \cos(2\pi x_i)] \quad (37)$$

Rosenbrock function

$$f(x) = (1 - x_1)^2 + 100(x_2 - x_1^2)^2 \quad (38)$$

Schaffer No.2 function

$$f(x) = 0.5 + \frac{\sin^2(x_1^2 - x_2^2) - 0.5}{(1 + 0.001(x_1^2 + x_2^2))^2} \quad (39)$$

Schaffer No.6 function

$$f(x) = 0.5 + \frac{\sin^2 \sqrt{x_1^2 + x_2^2} - 0.5}{(1 + 0.001(x_1^2 + x_2^2))^2} \quad (40)$$

Schwefel function

$$f(x) = 418.9829n - \sum_{i=1}^n \left[x_i \sin(\sqrt{|x_i|}) \right] \quad (41)$$

Shekel n.5 function

$$f(x) = - \sum_{j=1}^5 \left[c_j + \sum_{i=1}^4 (x_i - A_{i,j})^2 \right]^{-1} \quad (42)$$

with

$$c = \frac{1}{10} [1 \ 2 \ 2 \ 4 \ 4]^T \quad A = \begin{bmatrix} 4 & 1 & 8 & 6 & 3 \\ 4 & 1 & 8 & 6 & 7 \\ 4 & 1 & 8 & 6 & 3 \\ 4 & 1 & 8 & 6 & 7 \end{bmatrix}^T$$

Shekel n.7 function

$$f(x) = - \sum_{j=1}^7 \left[c_j + \sum_{i=1}^4 (x_i - A_{i,j})^2 \right]^{-1} \tag{43}$$

with

$$c = \frac{1}{10} [1 \ 2 \ 2 \ 4 \ 4 \ 6 \ 3]^T \quad A = \begin{bmatrix} 4 & 1 & 8 & 6 & 3 & 2 & 5 \\ 4 & 1 & 8 & 6 & 7 & 9 & 5 \\ 4 & 1 & 8 & 6 & 3 & 2 & 3 \\ 4 & 1 & 8 & 6 & 7 & 9 & 3 \end{bmatrix}^T$$

Shekel n.10 function

$$f(x) = - \sum_{j=1}^{10} \left[c_j + \sum_{i=1}^4 (x_i - A_{i,j})^2 \right]^{-1} \tag{44}$$

with

$$c = \frac{1}{10} [1 \ 2 \ 2 \ 4 \ 4 \ 6 \ 3 \ 7 \ 5 \ 5]^T$$

$$A = \begin{bmatrix} 4 & 1 & 8 & 6 & 3 & 2 & 5 & 8 & 6 & 7 \\ 4 & 1 & 8 & 6 & 7 & 9 & 5 & 1 & 2 & 3.6 \\ 4 & 1 & 8 & 6 & 3 & 2 & 3 & 8 & 6 & 7 \\ 4 & 1 & 8 & 6 & 7 & 9 & 3 & 1 & 2 & 3.6 \end{bmatrix}^T$$

Shubert penalty 1 function

$$f(x) = \prod_{i=1}^2 \left(\sum_{j=1}^5 j \cos((j+1)x_i + j) \right) + \left((x_1 + 1.42513)^2 + (x_2 + 0.80032)^2 \right) / 2 \tag{45}$$

Shubert penalty 2 function

$$f(x) = \prod_{i=1}^2 \left(\sum_{j=1}^5 j \cos((j+1)x_i + j) \right) + (x_1 + 1.42513)^2 + (x_2 + 0.80032)^2 \tag{46}$$

Six-humps Camel Back function

$$f(x) = \left(4 - 2.1x_1^2 + \frac{1}{3}x_1^4\right)x_1^2 + x_1x_2 + (4x_2^2 - 4)x_2^2 \quad (47)$$

Sphere function

$$f(x) = \sum_{i=1}^n x_i^2 \quad (48)$$

Styblinski–Tang function

$$f(x) = \frac{1}{2} \sum_{i=1}^n (x_i^4 - 16x_i^2 + 5x_i) \quad (49)$$

Test Tube Holder function

$$f(x) = -4 \left| e^{\left| \cos\left(\frac{1}{200}x_1^2 + \frac{1}{200}x_2^2\right) \right|} \sin(x_1) \cos(x_2) \right| \quad (50)$$

Three-humps Camel Back function

$$f(x) = 2x_1^2 - 1.05x_1^4 + \frac{1}{6}x_1^6 + x_1x_2 + x_2^2 \quad (51)$$

Treccani function

$$f(x) = x_1^4 + 4x_1^3 + 4x_1^2 + x_2^2 \quad (52)$$

Tripod function

$$\begin{aligned} f(x) = & \frac{1 - \text{sign}(x_2)}{2} (|x_1| + |x_2 + 50|) \\ & + \frac{1 + \text{sign}(x_2)}{2} \frac{1 - \text{sign}(x_1)}{2} (1 + |x_1 + 50| + |x_2 - 50|) \\ & + \frac{1 + \text{sign}(x_2)}{2} \frac{1 + \text{sign}(x_1)}{2} (2 + |x_1 - 50| + |x_2 - 50|) \end{aligned} \quad (53)$$

with

$$\text{sign}(x_i) = \begin{cases} -1, & \text{if } x_i \leq 0 \\ 1, & \text{else} \end{cases}$$

References

- Audet C, Dennis JE Jr (2006) Mesh adaptive direct search algorithms for constrained optimization. *SIAM J Optim* 17(1):188–217
- Audet C, Bécharad V, Le Digabel S (2008) Nonsmooth optimization through mesh adaptive direct search and variable neighborhood search. *J Glob Optim* 41(2):299–318
- Bartholomew-Biggs MC, Parkhurst SC, Wilson SP (2002) Using DIRECT to solve an aircraft routing problem. *Comput Optim Appl* 21(3):311–323
- Bassanini P, Bulgarelli U, Campana E, Lalli F (1994) The wave resistance problem in a boundary integral formulation. *Surv Math Ind* 4:151–194
- Campana E, Peri D, Tahara Y, Stern F (2006) Shape optimization in ship hydrodynamics using computational fluid dynamics. *Comput Methods Appl Mech Eng* 196(1–3):634–651
- Chen X, Diez M, Kandasamy M, Zhang Z, Campana EF, Stern F (2015) High-fidelity global optimization for shape design by dimensionality reduction, metamodels and particle swarm. *Eng Optim* 47(4):473–494
- Chiter L (2006) DIRECT algorithm: a new definition of potentially optimal hyperrectangles. *Appl Math Comput* 179(2):742–749
- Deb K, Pratap A, Agarwal S, Meyarivan T (2002) A fast and elitist multiobjective genetic algorithm: NSGA-II. *IEEE Trans Evolut Comput* 6(2):182–197
- Di Serafino D, Liuzzi G, Piccialli V, Riccio F, Toraldo G (2011) A modified DIviding RECTangles algorithm for a problem in astrophysics. *J Optim Theory Appl* 151(1):175–190
- Diez M, Iemma U (2012) Multidisciplinary conceptual design optimization of aircraft using a sound-matching-based objective function. *Eng Optim* 44(5):591–612
- Diez M, Peri D, Fasano G, Campana EF (2012) Hydroelastic optimization of a keel fin of a sailing boat: a multidisciplinary robust formulation for ship design. *Struct Multidiscip Optim* 46(4):613–625
- Diez M, Campana EF, Stern F (2015a) Design-space dimensionality reduction in shape optimization by Karhunen–Loève expansion. *Comput Methods Appl Mech Eng* 283:1525–1544
- Diez M, Serani A, Campana E, Goren O, Sarioz K, Danisman D, Grigoropoulos G, Aloniati E, Visonneau M, Queutey P, Stern F (2015b) Multi-objective hydrodynamic optimization of the DTMB 5415 for resistance and seakeeping. In: *Proceedings of the 13th international conference on fast sea transportation, FAST 2015, Washington, DC*
- Duddeck F (2008) Multidisciplinary optimization of car bodies. *Struct Multidiscip Optim* 35(4):375–389
- Gablonsky J, Kelley C (2001) A locally-biased form of the DIRECT algorithm. *J Glob Optim* 21(1):27–37
- He J, Watson L, Ramakrishnan N, Shaffer C, Verstak A, Jiang J, Bae K, Tranter W (2002) Dynamic data structures for a direct search algorithm. *Comput Optim Appl* 23(1):5–25
- He J, Verstak A, Watson L, Sosonkina M (2008) Design and implementation of a massively parallel version of DIRECT. *Comput Optim Appl* 40:217–245
- He J, Verstak A, Watson L, Sosonkina M (2009a) Performance modeling and analysis of a massively parallel DIRECT—part 1. *Int J High Perform Comput Appl* 23:14–28
- He J, Verstak A, Watson L, Sosonkina M (2009b) Performance modeling and analysis of a massively parallel DIRECT—part 2. *Int J High Perform Comput Appl* 23:29–41
- Hojjat M, Stavropoulou E, Bletzinger KU (2014) The vertex morphing method for node-based shape optimization. *Comput Methods Appl Mech Eng* 268:494–513
- Irvine M Jr, Longo J, Stern F (2008) Pitch and heave tests and uncertainty assessment for a surface combatant in regular head waves. *J Ship Res* 52(2):146–163
- Jones D (2009) DIRECT global optimization. In: *Pardalos PM, Floudas CA (eds) Encyclopedia of optimization*. Springer, Berlin, pp 725–735
- Jones D, Perttunen C, Stuckman B (1993) Lipschitzian optimization without the Lipschitz constant. *J Optim Theory Appl* 79(1):157–181
- Kandasamy M, Peri D, Tahara Y, Wilson W, Miozzi M, Georgiev S, Milanov E, Campana EF, Stern F (2013) Simulation based design optimization of waterjet propelled Delft catamaran. *Int Shipbuild Progr* 60(1):277–308
- Kandasamy M, Wu P, Zalek S, Karr D, Bartlett S, Nguyen L, Stern F (2014) CFD based hydrodynamic optimization and structural analysis of the hybrid ship hull. *SNAME Trans (To appear)*
- Kirkpatrick S (1984) Optimization by simulated annealing: quantitative studies. *J Stat Phys* 34(5–6):975–986

- Kirkpatrick S, Gelatt CD Jr, Vecchi MP (1983) Optimization by simulated annealing. *Science* 220(4598):671–680
- Kolda TG, Lewis RM, Torczon V (2003) Optimization by direct search: new perspectives on some classical and modern methods. *SIAM Rev* 45(3):385–482
- Kotinis M, Kulkarni A (2012) Multi-objective shape optimization of transonic airfoil sections using swarm intelligence and surrogate models. *Struct Multidiscip Optim* 45(5):747–758
- Liuzzi G, Lucidi S, Piccialli V (2010) A DIRECT-based approach exploiting local minimizations for the solution of large-scale global optimization problems. *Comput Optim Appl* 45:353–375
- Liuzzi G, Lucidi S, Piccialli V (2015) Exploiting derivative-free local searches in DIRECT-type algorithms for global optimization. *Comput Optim Appl*. doi:10.1007/s10589-015-9741-9
- Longo J, Stern F (2005) Uncertainty assessment for towing tank tests with example for surface combatant DTMB model 5415. *J Ship Res* 49(1):55–68
- Lucidi S, Sciandrone M (2002) A derivative-free algorithm for bound constrained optimization. *Comput Optim Appl* 21(2):119–142
- Moré J, Wild S (2009) Benchmarking derivative-free optimization algorithms. *SIAM J Optim* 20(1):172–191
- Olivieri A, Pistani F, Avanzini A, Stern F, Penna R (2001) Towing tank experiments of resistance, sinkage and trim, boundary layer, wake, and free surface flow around a naval combatant INSEAN 2340 model. Technical report, DTIC Document
- Papanikolaou A (2010) Holistic ship design optimization. *Comput-Aided Des* 42(11):1028–1044
- Schillings C, Schmidt S, Schulz V (2011) Efficient shape optimization for certain and uncertain aerodynamic design. *Comput Fluids* 46(1):78–87
- Schlichting H, Gersten K (2000) *Boundary-layer theory*. Springer, Berlin
- Serani A, Diez M, Leotardi C, Peri D, Fasano G, Iemma U, Campana E (2014) On the use of synchronous and asynchronous single-objective deterministic particle swarm optimization in ship design problems. In: *Proceedings of the 1st international conference in engineering and applied sciences optimization*, Kos
- Serani A, Fasano G, Liuzzi G, Lucidi S, Iemma U, Campana EF, Diez M (2015) Derivative-free global design optimization in ship hydrodynamics by local hybridization. In: *Proceedings of COMPIT, 14th international conference on computer applications and information technology in the maritime industries, 2015*, Ulrichshusen
- Stern F, Longo J, Penna R, Olivieri A, Ratcliffe T, Coleman H (2000) International collaboration on benchmark CFD validation data for surface combatant DTMB model 5415. In: *Proceedings of the twenty-third symposium on naval hydrodynamics*, Val de Reuil
- Tahara Y, Peri D, Campana E, Stern F (2008) Computational fluid dynamics-based multiobjective optimization of a surface combatant using a global optimization method. *J Mar Sci Technol* 13:95–116
- Telste J, Reed A (1994) Calculation of transom stern flows. In: *Proceedings of the sixth international conference on numerical ship hydrodynamics*, pp 78–92
- Volpi S, Diez M, Gaul NJ, Song H, Iemma U, Choi K, Campana EF, Stern F (2015) Development and validation of a dynamic metamodel based on stochastic radial basis functions and uncertainty quantification. *Struct Multidiscip Optim* 51(2):357–368
- Wang H, Lia G, Lib E (2010) Time-based metamodeling technique for vehicle crashworthiness optimization. *Comput Methods Appl Mech Eng* 199:2497–2509
- Zhu H, Bogy D (2002) DIRECT algorithm and its application to slider air-bearing surface optimization. *IEEE Trans Magn* 38(5):2168–2170